Optics Communications 282 (2009) 473–477

Contents lists available at ScienceDirect

Optics Communications

journal homepage: www.elsevier.com/locate/optcom

Overall second-order parametric characterization of light beams propagating through spiral phase elements

R. Martínez-Herrero *, A. Manjavacas

Departamento de Óptica, Universidad Complutense de Madrid, 28040 Madrid, Spain

ARTICLE INFO

Article history:
Received 22 July 2008
Received in revised form 9 October 2008
Accepted 30 October 2008

ABSTRACT

In terms of the spiral spectrum of the light beams, second-order irradiance moments of partially polarized, partially coherent beams are considered. We investigate the effects generated by spiral phase elements on the beam size, divergence and waist-plane position of the field. Attention is also focused on the beam quality parameter. These results are applied to several types of depleted-center (doughnut-shape) beams.

1. Introduction

As is well known, beam shaping refers to obtaining a prescribed beam structure from a given light field. In a general case, this procedure would handle the phase, irradiance and polarization distributions throughout the beam cross-section. Consequently, local beam shaping constitutes a rather involved task because the transverse profile of the field should be altered, in a controlled way, at each point. Instead, in the present work we are interested on overall changes, characterized by means of certain parameters and figures of merit that globally describe the spatial structure of the beam. More specifically, we are concerned with the irradiance moments of the field, which have been extensively investigated in the literature [1–6] and some of them adopted as ISO standards. In particular, we focus our attention in the present paper on the main irradiance moments, namely, the beam size, the far-field divergence, the waist-plane position and the beam quality parameter.

In general, the beam control can be implemented by using either intracavity devices or extracavity non-ABCD optical systems [7–13]. In this paper, attention will be focused on the so-called spiral phase elements (SPEs) [9–11,13]. The increasing interest on this type of optical device arises from its use in connection with certain depleted-center beams such as those employed in trapping of microscopic particles [14,15], focusing of atomic beams [16], and digital spiral imaging [17,18], which are well described by means of their spiral spectrum.

Within such framework, the aim of this paper is to analyse and characterize the second-order overall changes suffered by partially-polarized and partially-coherent fields travelling along SPEs. This paper is then arranged as follows. In the next section, the general formalism and the key definitions to be used in the rest of the work are introduced. In Section 3, the beam size, far-field divergence and waist position are expressed in terms of the spiral spectrum of a field. Section 4 considers how the beam quality parameter is altered after crossing an SPE. Application of the above results to some illustrative examples of depleted-center beams is given in Section 5. Finally, the main conclusions are summarized in Section 6.

2. Formalism and key definitions

Let us consider a statistically stationary light beam propagating along the z-axis. Assuming the quasi-transversality condition within the paraxial approach, the associated transverse electrical field vector at frequency ω, can be written in the form

$$\mathbf{E}(\mathbf{r}, z, \omega) = (E_s(\mathbf{r}, z, \omega), E_p(\mathbf{r}, z, \omega), 0), \quad (1)$$

where the subscripts s and p refer to the Cartesian components orthogonal to z, and $\mathbf{r} = (x,y)$ denotes the position vector at plane z = constant. For simplicity, the explicit dependence on ω will be omitted from now on. The coherent-polarization properties of such field can then be characterized by the so-called cross-spectral density tensor, represented by a 2×2 matrix whose elements are [19]

$$W_{ij}(\mathbf{r}_1, \mathbf{r}_2, z) = \overline{E_i^*(\mathbf{r}_1, z) E_j(\mathbf{r}_2, z)}, \quad i, j = s, p, \quad (2)$$

where * denotes the complex conjugate and the overbar symbolizes averaging over an ensemble of field realization. Here we are interested in the description of the spatial structure of the beam profile by means of certain overall parameters, namely, the so-called second-order beam moments, well-known and extensively analysed [1–8,20–22]. In the vectorial case, the main ones can be defined in the form [23–25]

* Corresponding author. Fax: +34 91 394 4683.
E-mail address: r.m-h@fis.ucm.es (R. Martínez-Herrero).

0030-4018/$ - see front matter
doi:10.1016/j.optcom.2008.10.071

$$\langle r^2\rangle = \frac{I_s}{I}\langle r^2\rangle_s + \frac{I_p}{I}\langle r^2\rangle_p, \quad (3)$$

$$\langle \eta^2\rangle = \frac{I_s}{I}\langle \eta^2\rangle_s + \frac{I_p}{I}\langle \eta^2\rangle_p, \quad (4)$$

$$\langle \mathbf{r}\cdot\boldsymbol{\eta}\rangle = \frac{I_s}{I}\langle \mathbf{r}\cdot\boldsymbol{\eta}\rangle_s + \frac{I_p}{I}\langle \mathbf{r}\cdot\boldsymbol{\eta}\rangle_p, \quad (5)$$

where $k\eta = (ku,kv) = (k_x,k_y)$ gives the wave vector components along the x- and y-axis, and

$$\langle \xi\varsigma\rangle_j = \frac{1}{I_j}\frac{k^2}{4\pi^2}\int\int\int \xi\varsigma\overline{E_j^*(\mathbf{r}+\mathbf{s}/\mathbf{2},z)E_j(\mathbf{r}-\mathbf{s}/\mathbf{2},z)} \times \exp(ik\mathbf{s}\cdot\boldsymbol{\eta})d\mathbf{s}\,d\mathbf{r}\,d\boldsymbol{\eta}, \quad j=s,p, \quad \xi,\varsigma = x,y,u,v \quad (6)$$

being

$$I_j = \int\int \overline{|E_j(\mathbf{r})|^2}d\mathbf{r}, \quad j=s,p, \quad (7)$$

the total power associated to the j component. Note that u and v would represent angles of propagation (without taking the evanescent waves into account). It should be remarked, in addition, that the four first-order moments, $\langle x\rangle$, $\langle y\rangle$, $\langle u\rangle$ and $\langle v\rangle$, define the center of the beam and its mean direction. For simplicity, in what follows we will assume that these moments equal zero (this is not a restriction since is equivalent to a shift of the Cartesian coordinate system).

As is well known [1,2,4,24], the second-order moments defined by Eqs. (3)–(5) are shown to be closely related with the overall spatial structure of the beam. In fact, they exhibit clear physical meaning, which can be summarized as follows:

– $\langle r^2\rangle$ represents the (square) beam width at the plane z = constant, i.e., the spatial size of the cross-section where the intensity takes significant values.
– $\langle \eta^2\rangle$ gives a measure of the (squared) far-field divergence, which is connected with the energy distribution associated with each spatial frequency of the beam.
– $\langle \mathbf{r}\cdot\boldsymbol{\eta}\rangle$ is related to the average of the curvature radius of the global beam. Moreover, it gives the position of the beam waist, i.e., the plane where the beam width takes its minimum value. More specifically, $\langle \mathbf{r}\cdot\boldsymbol{\eta}\rangle$ vanishes at such plane.

It is also interesting to note that the Rayleigh range z_R [24] (which represent the distance, from the waist, that the beam must freely propagate to duplicate its square width) can be expressed in terms of the irradiance moments in the form

$$z_R = \left(\frac{\langle r^2\rangle_w}{\langle \eta^2\rangle}\right)^{1/2}, \quad (8)$$

where the subscript w indicates the transverse size at the waist plane.

To get a joint description of the focusing and collimation capabilities of a light field we will handle the so-called beam quality parameter Q [23,24], which, in the vectorial case, takes the form

$$Q = \langle r^2\rangle\langle \eta^2\rangle - \langle \mathbf{r}\cdot\boldsymbol{\eta}\rangle^2, \quad (9)$$

where the moments are defined in Eqs. (3) and (5). This parameter Q exhibits a number of practical properties. Let us mention two of them:

– Q remains invariant under propagation through rotationally-symmetric ABCD optical systems (including rotation of the transverse coordinate axes).
– $Q \geq \frac{1}{k^2}$, where the equality is reached for uniformly polarized Gaussian beams.

Small values of parameter Q mean high focusability (small beam width) along with low beam divergence at the far field. It is important to remark that, in the vectorial case, the beam quality parameter does not reduce to the sum of the beam quality parameters, Q_s and Q_p, associated to the s- and p-components, respectively. In fact, we obtain from Eqs. (3)–(5) and (9)

$$Q = \left(\frac{I_s}{I}\right)^2 Q_s + \left(\frac{I_p}{I}\right)^2 Q_p + \frac{I_sI_p}{I^2}Q_{sp}, \quad (10)$$

where

$$Q_j = \langle r^2\rangle_j\langle \eta^2\rangle_j - \langle \mathbf{r}\cdot\boldsymbol{\eta}\rangle_j^2, \quad j=s,p \quad (11)$$

and the crossed term Q_{sp} is given by

$$Q_{sp} = \langle r^2\rangle_s\langle \eta^2\rangle_p + \langle r^2\rangle_p\langle \eta^2\rangle_s - 2\langle \mathbf{r}\cdot\boldsymbol{\eta}\rangle_s\langle \mathbf{r}\cdot\boldsymbol{\eta}\rangle_p. \quad (12)$$

3. Second-order moments in terms of the spiral spectrum

As we pointed out in the Introduction, the so-called spiral spectrum of the field has revealed to be a useful tool to handle certain kind of beams. For the sake of convenience (which will be apparent later), let us write the second-order moments in terms of the spiral spectrum of the field. Thus we expand the electric field at a transverse plane (say, z = 0) as follows:

$$\mathbf{E}(R,\theta) = \sum_n \mathbf{E}_n(R)\exp(in\theta), \quad j=s,p, \quad (13)$$

where R and θ denote the polar coordinates at plane z = 0, and

$$\mathbf{E}_n(R) = \frac{1}{2\pi}\int_0^{2\pi}\mathbf{E}(R,\theta)\exp(-in\theta)d\theta, \quad (14)$$

It should be remarked that the weight of mode n in the spiral spectrum is given by

$$c_n = 2\pi\int_0^\infty \overline{|\mathbf{E}_n(R)|^2}RdR. \quad (15)$$

For the sake of simplicity, in the remainder of this paper, we choose the s- and p-axis in such a way that $I_s = I_p = I$. This choice is always possible because it only involves a suitable axes rotation [22].

Taking into account the spiral spectrum decomposition (Eq. (13)), the second-order moments become

$$\langle r^2\rangle = \frac{\pi}{I}\sum_n\int_0^\infty \overline{|\mathbf{E}_n(R)|^2}R^3dR, \quad (16)$$

$$\langle \eta^2\rangle = \frac{\pi}{k^2I}\sum_n\int_0^\infty \overline{|\mathbf{E}'_n(R)|^2}RdR + \frac{\pi}{k^2I}\sum_n n^2\int_0^\infty \overline{|\mathbf{E}_n(R)|^2}\frac{1}{R}dR, \quad (17)$$

$$\langle \mathbf{r}\cdot\boldsymbol{\eta}\rangle = \frac{\pi}{ikI}\sum_n \times\int_0^\infty\left[\overline{E'_{ns}(R)E^*_{ns}(R) - E'^*_{ns}(R)E_{ns}(R) + E'_{np}(R)E^*_{np}(R) - E'^*_{np}(R)E_{np}(R)}\right]RdR \quad (18)$$

where the prime means derivation with respect to R.

From these expressions, we conclude that each one of the second-order moments can be understood as the sum of the corresponding moments associated to the spiral spectrum components (apart from the weight of each mode, c_n). In order to go further into Eqs. (16)–(18), let us consider two singlemode fields, namely, $\mathbf{E}_1$ and $\mathbf{E}_2$, with the same spatial structure at z = 0,

$$\mathbf{E}_1(R,\theta) = \mathbf{E}_0(R)\exp(in\theta), \quad (19a)$$

$$\mathbf{E}_2(R,\theta) = \mathbf{E}_0(R)\exp(im\theta), \quad (n\neq m) \quad (19b)$$

where $\mathbf{E}_0$ contains the information about the polarization and the R-dependence of the fields. From Eqs. (16)–(18), it can be shown that

$$\langle r^2\rangle_1 = \langle r^2\rangle_2 \equiv \langle r^2\rangle, \tag{20a}$$
$$\langle \eta^2\rangle_1 - \langle \eta^2\rangle_2 = (n^2 - m^2)M, \tag{20b}$$
$$\langle \mathbf{r}\cdot\boldsymbol{\eta}\rangle_1 = \langle \mathbf{r}\cdot\boldsymbol{\eta}\rangle_2, \tag{20c}$$

where

$$M = \frac{\pi}{k^2 I}\int_0^\infty \frac{\overline{|\mathbf{E}_0(R)|^2}}{R}dR \tag{21}$$

with $I = 2\pi\int_0^\infty \overline{|\mathbf{E}_0(R)|^2}RdR$. We see that the different behaviour of the above field modes is shown only through the value of the far-field divergence. Consequently, the beam waists are placed at different planes and, in addition, the Rayleigh length also differs for both fields. Concerning the beam quality, it can be found at once

$$Q_1 - Q_2 = \langle r^2\rangle(n^2 - m^2)M. \tag{22}$$

We conclude from Eq. (22) that for singlemode fields with the same transversal spatial and polarization structure, the beam quality increase when the order of the mode increases as well: High-order modes have worse beam quality. It can also be shown that, when $m \neq 0$, the best quality (lower Q) corresponds to the uniformly polarized beam, whose dimensionless amplitude, A, at $z = 0$ is

$$A = \left(\frac{R}{\omega_0}\right)^m \exp\left(-\frac{R^2}{\omega_0^2}\right), \tag{23}$$

where ω_0 being a constant. Of course, for $m = 0$, the best quality corresponds to the typical uniformly polarized Gaussian beam.

4. Beam quality changes after propagation through spiral phase elements

Let us now assume that a light beam passes through a spiral phase element. This device will adds a spiral phase $\varphi = p\theta$ to the field amplitude. Accordingly, it can be shown that the relation between the second-order irradiance moments at the input and output planes of the SPE is given by

$$\langle r^2\rangle_o = \langle r^2\rangle_i, \tag{24}$$
$$\langle \mathbf{r}\cdot\boldsymbol{\eta}\rangle_o = \langle \mathbf{r}\cdot\boldsymbol{\eta}\rangle_i, \tag{25}$$
$$\langle \eta^2\rangle_o = \langle \eta^2\rangle_i + M_p, \tag{26}$$

where

$$M_p = \frac{\pi}{k^2 I}\sum_n (p^2 + 2np)\int_0^\infty \overline{|\mathbf{E}_n(R)|^2}\frac{1}{R}dR. \tag{27}$$

We see that the beam width $\langle r^2\rangle$ and the average curvature radii $\langle \mathbf{r}\cdot\boldsymbol{\eta}\rangle$ remain unchanged, as expected. However, the far-field divergence $\langle \eta^2\rangle$ is altered. Moreover, since the SPE introduces a change on the spiral spectrum of the field, the polarization behaviour is also modified upon free propagation [26].

At the output of the SPE, the quality parameter, Q_o, is obtained from Eq. (9):

$$Q_o = Q_i + \langle r^2\rangle_i M_p. \tag{28}$$

Taking this into account, we get for the ratio $\frac{Q_o - Q_i}{Q_i}$ the value

$$\frac{\Delta Q}{Q_i} \equiv \frac{Q_o - Q_i}{Q_i} = \frac{\langle r^2\rangle_i M_p}{Q_i}. \tag{29}$$

Thus, depending on the characteristics of the spiral spectrum, the SPE could improve or deteriorate the beam quality. In order to get further insight into this behavior, we will next analyse some illustrative examples.

5. Application to some depleted-center beams

Let us consider two different kind of beams. The first example is a uniformly-polarized doughnut-shape beam, $\mathbf{E}_1$, whose electric field amplitude reads at plane $z = 0$

$$\mathbf{E}_1(R,\theta) = g(R)\exp(i\theta)(a,b), \tag{30}$$

where a and b are stochastic variables that, in accordance with our previous assumption, satisfy the condition $\overline{|a|^2} = \overline{|b|^2} \equiv I_0$, and

$$g(R) = \frac{\sqrt{2}}{\omega_0}R\exp\left(-\frac{R^2}{\omega_0^2}\right). \tag{31}$$

Fig. 1 shows the irradiance distribution at $z = 0$, which is the plane where the SPE is placed. For this type of field, the well-known local degree of polarization, P, [19,27] becomes independent of the propagation distance z, and takes the value

$$P = \frac{\overline{a^* b}}{I_0}. \tag{32}$$

In particular, the input field is totally polarized when $\overline{a^* b} = I_0$, and becomes non-polarized if $\overline{a^* b} = 0$. Otherwise, the beam is (uniformly) partially polarized.

The beam quality at the input plane of the SPE reads

$$Q_i = \frac{4}{k^2}. \tag{33}$$

After travelling through this device, the quality parameter becomes

$$Q_o = \frac{2}{k^2}(p^2 + 2p + 2), \tag{34}$$

and we get for the ratio $\frac{\Delta Q}{Q_i}$ the value

$$\frac{\Delta Q}{Q_i} = \frac{p^2 + 2p}{2}. \tag{35}$$

Therefore, for this kind of fields, the beam quality factor is not improved unless $p = -1$. In such a case, we have

$$Q_o = \frac{2}{k^2}, \tag{36}$$
$$\frac{\Delta Q}{Q_i} = -\frac{1}{2}. \tag{37}$$

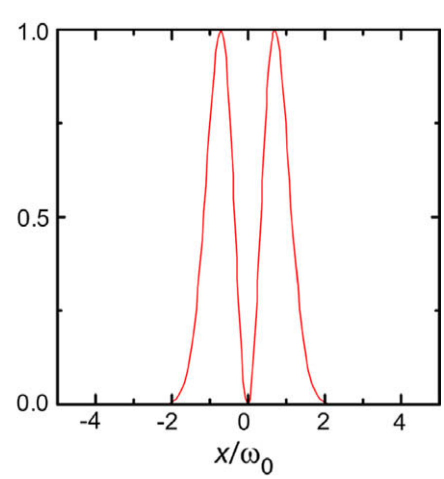

Fig. 1. Irradiance distribution at plane $z = 0$ for the two types of beams considered in Section 5 (cf. Eqs. (30) and (38)).

It should also be noted that there is no variation of the beam quality parameter when $p = -2$: This should be expected because the action of the SPE only produces changes from the harmonic with $n = 1$ to the one with $n = -1$ in the spiral spectrum.

Fig. 2 shows the far-field irradiance distributions in the absence of SPE (a) or with the passage through this device with $p = -1$ (b). We see that the presence of this SPE generates a bell-shape at the far field. Furthermore, as it was pointed out above, in both cases, (a) and (b), the degree of polarization of this beam remains unchanged.

The second example corresponds to a radially polarized doughnut-shape beam, $\mathbf{E}_2$, given by

$$\mathbf{E}_2(R,\theta) = g(R)\exp(i\theta)(\cos\theta, \sin\theta), \tag{38}$$

where $g(R)$ is also given by Eq. (31). The irradiance distribution associated to this field is identical to that of the first example, plotted in Fig. 1. The irradiance and the polarization diagram at the far field are plotted in Fig. 3a and c, respectively. We see that the field defined by Eq. (38) does not retain the radial character upon propagation into free space.

At the input and output planes of a SPE, we get for this field

$$Q_i = \frac{6}{k^2}, \tag{39}$$

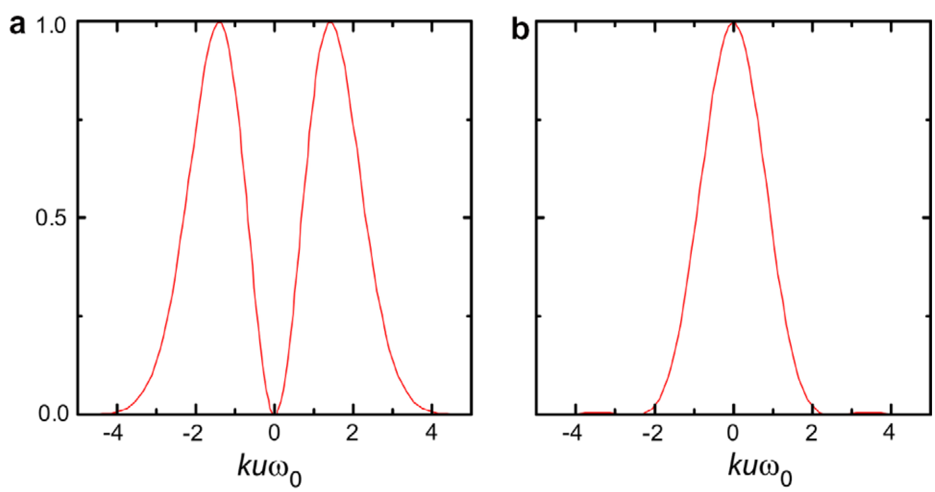

Fig. 2. Far-field irradiance distribution for the field defined in Eq. (30). In the figures $ku = k_x$ is the wave vector component of the beam. In (a) there is no SPE. In (b) the beam crosses through the SPE with $p = -1$. In both cases, the field remains uniformly polarized, and its degree of polarization P is given by Eq. (32).

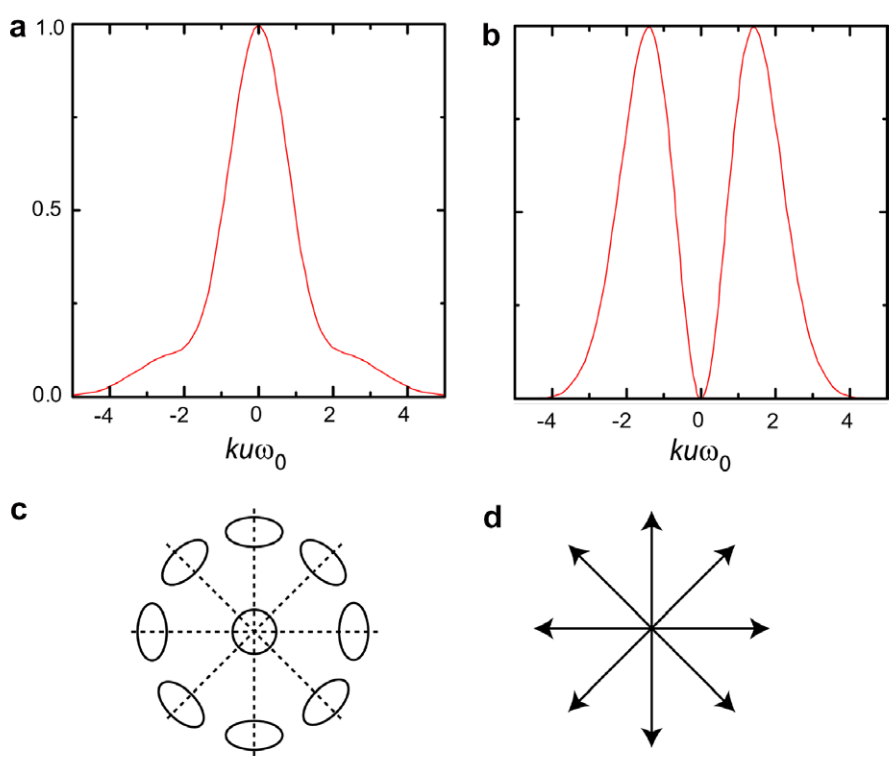

Fig. 3. Far-field irradiance (a and b) and polarization diagrams (c and d) for the field defined by Eq. (38). Again, $ku = k_x$ is the wave vector component of the beam. In (a) and (c) there is no SPE. In (b) and (d) the beam crosses through the SPE with $p = -1$. Note that in c the field is circularly polarized at the beam center. Furthermore, we see that when no SPE is present, the far-field polarization changes to a non-uniform elliptical pattern, whereas after passing through the SPE the field keeps its initial radial polarization.

and

$$Q_o = \frac{2}{k^2}(p^2 + 2p + 3). \quad (40)$$

Therefore, we obtain for this class of beams

$$\frac{\Delta Q}{Q_i} = \frac{p^2 + 2p}{3}. \quad (41)$$

We see again that the beam quality parameter is not improved unless $p = -1$. In this case,

$$Q_o = \frac{4}{k^2} \quad (42)$$

together with

$$\frac{\Delta Q}{Q_i} = -\frac{1}{3}. \quad (43)$$

Fig. 3b and d plot the irradiance and the polarization structure at the far field. We see that when the beam crosses through the SPE with $p = -1$, its radial polarization distribution is conserved under free propagation.

It should finally be remarked that, in both examples, the improvement of the beam quality is consistent with the results derived in previous papers [11,13].

6. Conclusions

The spiral spectrum of the light fields has revealed to be of practical use to analyse the main second-order irradiance moments in the vectorial case. The overall spatial structure of (paraxial) partially polarized, partially coherent beams can then be described in terms of the relative contribution of the modes of the spiral spectrum. This formalism also provides a simple way to determine how the beam is globally altered due to the presence of spiral phase elements. Two special depleted-center beams have been considered. In both cases, the local degree of polarization is uniform across the beam profile, and is preserved upon propagation into free space. In the first case, it has been shown that the action of a SPE with $p = -1$ produces a one-peak bell-shaped irradiance distribution at the far field. In the second example, use of this SPE allows to retain the radial-polarization structure under free propagation. In both cases, by means of a suitable choice of the SPE ($p = -1$), it has also been shown that the beam quality parameter can be improved.

Acknowledgements

This work has been supported by the Ministerio de Educación y Ciencia (MEC) of Spain, project FIS2007-63396, and by CM-UCN, Research Group Program 2008, No. 910335. One of the authors (A.M.) has a grant from the MEC. The authors would also like to thank Prof. P.M. Mejías for his interest and help.

References

[1] S. Lavi, R. Prochaska, E. Keren, Appl. Opt. 27 (1988) 3696.
[2] A.E. Siegman, Proc. SPIE 1224 (1990) 2.
[3] J. Serna, R. Martínez-Herrero, P.M. Mejías, J. Opt. Soc. Am. A 8 (1991) 1094.
[4] H. Weber, Opt. Quantum Electron. 24 (1992) 1027.
[5] R. Martínez-Herrero, P.M. Mejías, H. Weber, Opt. Quantum Electron. 25 (1993) 423.
[6] P.M. Mejías, R. Martínez-Herrero, Opt. Lett. 20 (1995) 660.
[7] R. Martínez-Herrero, P.M. Mejías, G. Piquero, Opt. Lett. 17 (1992) 1650.
[8] A.E. Siegman, Appl. Opt. 32 (1993) 5893.
[9] E. Abramochkin, N. Losevsky, V. Volostnikov, Opt. Commun. 141 (1997) 59.
[10] R. Oron, N. Davidson, A. Friesem, E. Hasman, Opt. Commun. 182 (2000) 205.
[11] R. Oron, N. Davidson, A. Friesem, E. Hasman, Opt. Lett. 25 (2000) 939.
[12] E. Miyai, K. Sakai, T. Okano, W. Kunishi, D. Ohnishi, S. Noda, Nature 441 (2006) 946.
[13] G. Machavarani, Y. Lumer, I. Moshe, S. Jackel, Opt. Commun. 271 (2007) 190.
[14] S. Sato, Y. Harada, Y. Waseda, Opt. Lett. 19 (1994) 1807.
[15] T. Kuga, Y. Torii, N. Shiokawa, T. Hirano, Phys. Rev. Lett. 78 (1997) 4713.
[16] J.J. McCelland, M.R. Scheinfein, J. Opt. Soc. Am. B 8 (1991) 1974.
[17] L. Torner, J. Torres, S. Carrasco, Opt. Express 13 (2005) 873.
[18] G. Molina-Terriza, L. Rebane, J.P. Torres, L. Torner, S. Carrasco, J. Eur. Opt. Soc. Rap. Public. 2 (2007) 07014.
[19] L. Mandel, E. Wolf, Optical Coherence and Quantum Optics, Cambridge University Press, Cambridge, 1995.
[20] R. Martínez-Herrero, P.M. Mejías, N. Hodgson, H. Weber, IEEE J. Quantum Electron. 31 (1995) 2173.
[21] F. Encinas-Sanz, J. Serna, C. Martínez, R. Martínez-Herrero, P.M. Mejías, IEEE J. Quantum Electron. 34 (1998) 17.
[22] R. Martínez-Herrero, P.M. Mejías, J.M. Movilla, J. Opt. Soc. Am. A 22 (2005) 1442.
[23] Q. Lü, S. Dong, H. Weber, Opt. Quantum Electron. 27 (1995) 777.
[24] P.M. Mejías, R. Martínez-Herrero, G. Piquero, J.M. Movilla, Prog. Quantum Electron. 26 (2002) 65.
[25] R. Martínez-Herrero, G. Piquero, P.M. Mejías, Opt. Commun. 281 (2008) 756.
[26] R. Martínez-Herrero, P.M. Mejías, Opt. Express 16 (2008) 9021.
[27] C. Brosseau, Fundamentals of Polarized Light, Wiley, New York, 1998.